Pulse Polarization for Li-Ion Battery under Constant State of Charge: Part I. Pulse Discharge Experiments

Tyler DuBeshter and Jacob Jorne[*,z]

Department of Chemical Engineering, University of Rochester, Rochester, New York 14627, USA

Given the increased dependence on battery-powered devices, it is necessary to develop new and robust methods to evaluate and predict battery performance and state of charge. Batteries, including Li-Ion batteries, are unsteady state systems and a need exists to evaluate performance under constant state of charge (SOC). The purpose of this work was to develop pulse polarization curves (PPC) for a Li-Ion battery under constant SOC in order to identify individual overvoltages, such as charge transfer kinetics and mass transport, and their SOC dependence. Consequently, we elected to conduct pulse discharges at various duration and discharge current densities, under well maintained SOCs. Based on the results we were able to construct pulse polarization curves for constant SOCs of 10, 40 and 70% at various pulse durations of 2, 10 and 30 seconds. The experimentally obtained pulse polarizations suggest that the kinetic overpotential is captured in the 2 second pulse, while electrolyte Li+ concentration and Li solid state diffusion gradients are established in the 10 and 30 second pulse times, respectively. This allowed us to identify the individual overvoltages experimentally. An important consideration was that as the battery's SOC changes, the open circuit voltage (OCV) also changes. Therefore, the pulse discharge method we used needed to end at the same SOC in all cases to enable the construction of a PPC with the same OCV. To ensure that this method applied to various sizes and chemistries of batteries reliably, we ran pulse discharge experiments on a high Amp hour (15 Ah) large Li-Ion pouch battery (power) that used a NMC LMO cathode, as well as on a low Amp hour (0.04 Ah) small electrode coin battery (energy) with a CoO_2 cathode. In a subsequent paper we employed the Newman method to model the pulse discharges, allowing prediction of the performance of Li-Ion batteries and constructing their PPCs under constant SOC.

Batteries operate in an unsteady state as properties and dimensions vary with time and state of charge (SOC). This presents a challenge to analyze battery performance, as the voltage-current polarization likewise varies with the SOC. In the Lithium Ion Battery (LIB), the charge transfer kinetics, ionic mass transport, and solid-state diffusion are coupled and determine overall battery voltage performance. Studying battery voltage vs. current density[1–5] has been and remains difficult, since the SOC changes when the battery is charging or discharging. No method, known to the authors, exists to evaluate the voltage vs. current density relationship at a constant SOC in a battery. However, there are several methods[1–6] to evaluate SOC and predict performance. Notably these include Bernardi's pulse discharge method[3] and Wijewardana's method to estimate SOC,[5] as well as others. Battery performance, voltage loss evolution, and separation of overvoltage losses depend on the identification of a method to evaluate these variables, which would be invaluable to the analysis and the improvement of batteries.

Fuel cells[7,8] and flow batteries, in contrast, operate in a steady state, hence a method exists that enables the analysis of the voltage vs. current density polarization.[8] This enables the construction of a unique polarization curve independent of time and history. Understanding the voltage vs. current density relationship, or polarization curve, has led to the identification of factors governing performance for different operating conditions in fuel cells.[7,8] For instance, at low current density, the performance of a polymer electrolyte membrane fuel cell is governed by the positive electrode kinetic losses.[8]

In contrast to fuel cells, batteries are unsteady state systems. During the cycling of the battery, the physical, chemical, and spatial parameters vary with the state of charge (SOC). The present work is an attempt to adapt polarization curves from fuel cells to batteries in general, and to LIBs in particular.

The main objective of studying battery voltage vs. current density is to enable the understanding of governing factors for battery performance under various operating conditions and given SOCs. These include charge transfer kinetics, ionic mass transport, and solid-state diffusion. Additionally, the SOC's influence on battery performance and individual overvoltages are investigated as well.

Batteries comparison and methods of measurement.—In a lithium ion battery[2,9–13] during discharge the lithium ions de-intercalate from the negative electrode, move through the electrolyte and separator, and intercalate into the positive electrode, as shown schematically in Figure 1.

Commonly, C-rate is defined as the amount of current required to fully discharge a battery in an hour. It is based on both current and capacity. C-rate is a measure based on a constant current and nominal capacity. For example, 1 C for a battery with a capacity of 15 Ah would be 15 amperes and would fully discharge the battery in 1 hour. 2 C would be 30 amperes and discharge the battery in 0.5 hours, and 0.5 C would be 7.5 amperes and discharge the battery in 2 hours. Since this measure takes the battery's capacity into account when determining current demands, it has typically been the easiest metric to compare individual battery performance. A problem with this metric occurs when comparing different capacity batteries that have the same C-rate, but different current densities. In this case the
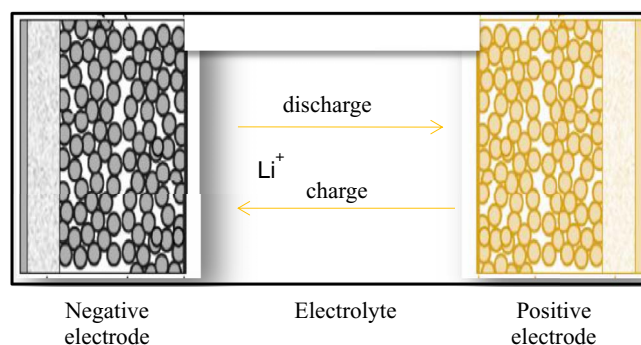

Figure 1. Schematic representation of a lithium-ion battery.

*Electrochemical Society Member.
zE-mail: jacob.jorne@rochester.edu

C-rate does not give an adequate comparison between the battery's performance metrics.

Pulse discharge and pulse polarization curve—The construction of a PPC for a battery under constant SOC is a challenge. Berndardi[3] had promising results utilizing a pulse discharge method to characterize performance, but since a battery is an unsteady state system, batteries exhibit different PPCs under varying SOCs.[3] To construct a PPC, one must maintain a constant ending SOC. To accomplish this, we used pulse discharges at a constant current and time, similar to that used by Bernardi,[3] but expanding SOC measurements to three distinct SOCs. By setting the SOC end condition, and modifying the SOC before the trial to include the total charge used during the pulse discharge, we were able to control the SOC at the end of the pulse.

The pulse discharge method was used to create PPCs for a LIB at various states of charge. By noting the voltage at the end of the pulse discharge for each current density, time, and SOC, we constructed PPCs at each SOC and discharge time scale. Experimentally, distinct PPCs were created at 10, 40, and 70% SOC for 2, 10, and 30 second pulse times. The current density range for these PPCs was $1/3$ C – $20/3$ C, or 0.5 mA/cm^2 to 10.9 mA/cm^2 for the large LIB pouch cell. The small coin cell was limited to 40% SOC, 10 second pulse discharge, and $1/3$ C to 2 C, or 3.5 mA/cm^2 to 20.8 mA/cm^2.

We then utilized the constructed curves to identify and separate the charge transfer kinetic, ionic mass transport, and solid-state diffusion contributions to the voltage loss at various SOCs. For a given SOC, the charge transfer kinetic, ionic mass transport, and solid-state diffusion voltage losses develop at different time scales. Consequently, we attempted to separate these overpotentials experimentally. The characteristic time scales can be estimated from the following approximation:

$$\tau_s = \frac{L^2}{D} \qquad [1]$$

where τ_s is the characteristic time, L is the characteristic length (thickness of a component) and D is the diffusion coefficient. From Equation 1, the charge transfer kinetic voltage losses[14–22] develop in 1 ms, Li$^+$ concentration gradient voltage losses in the electrolyte[19,20,23–30] develop in 5–10 seconds, and Li concentration gradient voltage losses in the solid-state diffusion[31–42] develop in 20–200 seconds. This is why we chose 2, 10, and 30 second pulse discharge times as the lengths to investigate experimentally.

Experimental Method for Pulse Polarization Curve Construction

Materials.—The pouch battery used for this experiment was the same one found in the first release of the Chevrolet Volt, and had a capacity of 15 Ah. Both the positive and negative electrode metal contacts were found on the same edge of the battery. The 16 positive and negative electrode tabs were welded together, respectively, and the battery assembly was sealed in an aluminized plastic pouch. The pouch battery was approximately 300 cm^2 and 1 cm thick, with each cell being approximately the same area, and about 150 microns thick when including the current collector thickness. The coin cell battery was smaller in capacity and physical size, with a capacity of 0.04 Ah and measuring approximately 3 cm^2 and 0.3 cm thick. The positive and negative electrodes are connected to the opposite faces of the battery respectively, as opposed to an edge. More detailed technical specifications of each battery are found in the following list.

Materials in the large pouch battery consisted of:

- Double coated 50 μm thick, graphite electrode on 10 μm Cu foil for the anode.
- Double coated 57 μm thick, Li-metal electrode (mixture of Li$_2$Mn$_2$O$_4$ and LiNi$_{0.3}$Mn$_{0.3}$Co$_{0.3}$O$_2$ on 20 μm thick Al foil for the cathode.
- 25 μm separator.
- 1 M LiPF$_6$ electrolyte in 1:1 ethylene carbonate EC and dimethyl carbonate DMC.
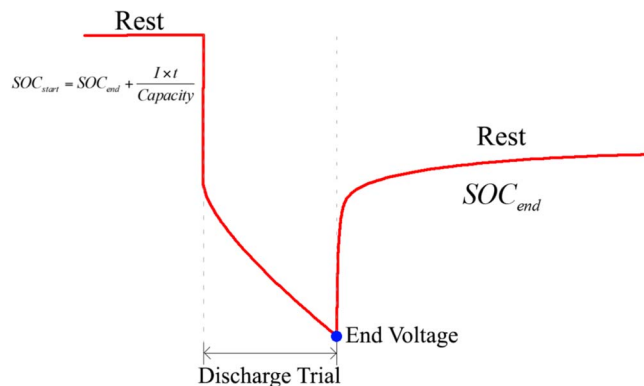- 285.18 cm^2 cross sectional area.

Figure 2. Schematic of pulse discharge experiment. The blue point was the voltage used to construct the pulse polarization curve for each pre-determined SOC.

- 16 dual sided electrodes in parallel for 32 cells total.
- ∼15 Ah pouch cell corresponding to ∼16.4 Ah/m^2 unit cell.
- Manufacturer battery operational limits 4.15 V to 2.5 V.

Materials in the small coin cell battery consisted of:[43]

- AA Portable Power Corp. LiR2032.
- Estimated ∼500 μm thick, graphite electrode for the anode.
- Estimated ∼500 μm thick, CoO$_2$ Li-metal oxide electrode for the cathode
- 3.14 cm^2 cross sectional area.
- Single sided electrode, one pair of electrodes.
- 0.032 Ah capacity corresponding to ∼102 Ah/m^2.
- Manufacturer battery operational limits 4.20 V to 3.00 V.

Pulse discharge method.—In order to ensure constant temperature, all experiments were conducted in a climate control chamber with multiple temperature sensors on the battery. For the pulse discharge, the discharge time is a variable.

Before the pulse discharge experiment could be conducted, an accurate measurement of the battery capacity needed to be performed. The operating voltage limits for the battery were 4.15 V and 2.5 V for 100% and 0% SOC respectively. Capacity was determined by discharging the battery from 4.15 V at a constant current of $\frac{C}{3}$, to 2.5 V. This capacity test was repeated at 1 C three times. The capacity was then determined from an average of the current counted during the three 1 C discharge cycles. This process was repeated for both large pouch and small coin batteries. As shown in Figure 2, the battery capacity was used in the calculation for each pulse discharge trial. The equation used to calculate the SOC before the trial is as follows:

$$SOC_{start} = SOC_{end} + \frac{It}{C} \qquad [2]$$

where SOC_{start} is the SOC at the beginning of the pulse discharge, SOC_{end} is the SOC at the end of pulse discharge, I is the constant current applied during the pulse discharge, t is the pulse discharge time, and C is the capacity of the battery.

All measurements and methods for the large pouch battery were conducted using an Agilent N3300A load bank powered by an Agilent E3633A power supply that were controlled by a computer running Labview 7.0. On the coin cell, all measurements were programmed in a MITS-Pro controlling an Arbin BT-2043 Battery Cycler. The battery voltage operating limits were set at 4.15 V and 2.5 V for 100% and 0% SOC respectively. To measure capacity we galvanostatically charged the battery at 1 C until a potential of 4.15 was reached, at which point charging switched to a potentiostatic mode and continued charging until the current dropped to one twentieth of the capacity of the battery.
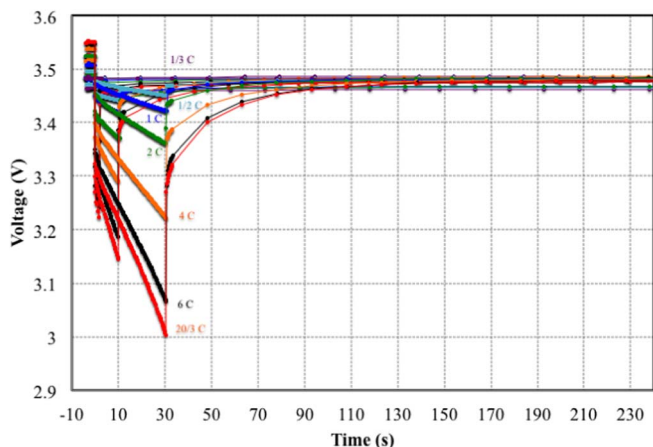
Figure 3. 10% SOC for all pulse discharge times and current densities for comparison between pulse discharge times.

Figure 4. 70% SOC, 30 s discharge pulse from 1/3 C to 20/3 C. The difference in OCV after relaxation is 25 mV 240 seconds after current interrupt.

The battery was set up for the pulse discharge experiment using a current counting method according to the following steps:

1) Galvanostatic charging to a potential of 4.15 V at 1 C, after which the load bank switched to potentiostatic mode to ensure a full charge to 4.15 V until the current approaches one twentieth of cell total capacity.
2) Cell rests for 15 minutes.
3) Discharging at a constant current of C/3 to a SOC as outlined in Figure 2.
4) Cell rests for 30 minutes.
5) Pulse discharge test begins at the specified current and time variables.
6) Cell rests for 60 minutes.
7) Repeat first step to charge cell to 100% SOC.

A schematic of steps 4, 5, and 6 is shown in Figure 2. In the schematic, it is shown how the SOC at the end of the pulse discharge is pre-determined, and the beginning SOC varies according to the pulse discharge trial being conducted. The SOC remained constant during the relaxation period. In this manner, we conducted pulse discharge experiments at 10%, 40%, and 70% SOC. For the large pouch cell, we tested at rates of C/3, C/2, 1 C, 2 C, 4 C, 6 C, and 6.67 C, and discharge times of 2, 10, and 30 seconds for each SOC. We repeated the pulse discharge experiment for the small coin cell at 40% SOC and 10 second discharge time, at C/3, C/2, 1 C, 3C/2, and 2 C. Construction of a PPC was accomplished by using the voltage at the end of the pulse (blue point) in Figure 2 for each current and time at the ending SOC for each battery. In this manner we could compare the effects of different discharge times, current densities, SOC, and chemistries on battery performance.

The pulse discharge experiments conducted here somewhat resemble that of GITT and PITT techniques which are commonly used in the battery community. The galvanostatic and potentiostatic intermittent titration techniques,[44] GITT and PITT respectively, have been used to estimate the solid-state diffusion coefficients for the electrodes in the lithium ion battery. The GITT method has been shown to be superior to the PITT method[44] in accurately determining the diffusion coefficient in an electrode, however both suffer some drawbacks when comparing to our proposed method. GITT uses a low current, typically C/10 or C/20, which takes a requisite longer time to test a battery when compared to our method which utilizes C/3 and higher. Our method attempts to experimentally separate the kinetic, electrolyte, and solid material voltage losses, in contrast with the GITT/PITT method which cannot estimate losses due to the electrolyte. While the GITT/PITT are able to determine diffusion in electrodes using half cells, our method can be more readily applied to many rechargeable commercial cells for performance evaluation and metrics. In a subsequent paper[46,47]
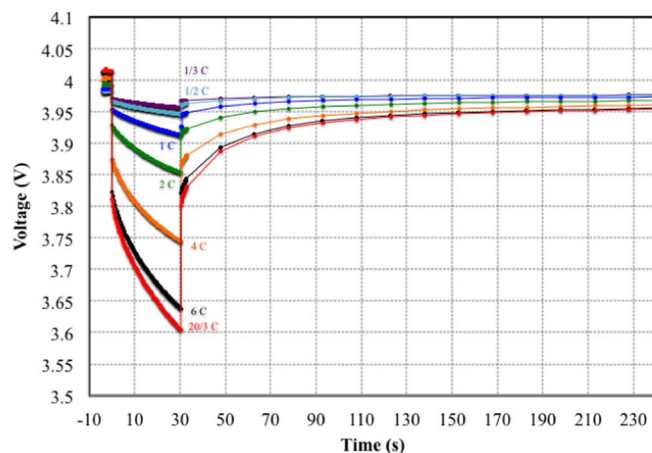
we utilized Newman's method to simulate the pulse discharge experiments and to extend the pulse time to 2–240 seconds in order to investigate steady state polarizations when all Lithium gradients are fully developed under constant SOC.

Results

Battery capacity measurements.—Following the first charge, the battery was discharged at C/3 from 5000 to 15000 seconds and the capacity was determined to be 14.72 A-hr. The following three charge/discharge cycles were performed at 1 C charge/discharge from 17000 to 47000 seconds approximately. The battery rested after both charge and discharge currents for fifteen minutes, allowing the battery to return to OCV. The average of these three 1 C discharge cycles were used to determine the capacity of the battery at 14.89 A-hr. The average capacity of the small coin cell following the same method was 0.032 A-hr, but with sixty minute rest periods.

Pulse discharge results.—The data for the pulse discharge experiments were grouped according to SOC and pulse discharge length. Each figure has the pulse discharge trials overlapping, to demonstrate the change in battery performance due to increased C-rate. We evaluated the effectiveness of our method to experimentally separate voltage loss contributions from these figures. Figures 3 and 4 are examples of typical pulse discharges for 10% SOC and 70% SOC, respectively.

The pulse discharge data for the 10% SOC trials at 2 second pulse discharges show that there is a slightly increased relaxation time experienced by the battery at progressively higher C-rates. This is expected, since the voltage losses due to kinetics were expected to develop within a one millisecond time scale, however our testing equipment was limited to a 2 second pulse discharge for the fastest pulse discharge time.

Figure 3 shows that for 10% SOC at 10 seconds pulse discharge the relaxation of the cell after the current interrupt is longer than the 2 second pulse. This is believed to correspond with a steady Li$^+$ concentration gradient in the electrolyte. Figure 3 is also believed to show the beginning of the solid state diffusion Li ion concentration gradient due to the relaxation time increasing significantly. As predicted, the majority of the pulse discharge relaxation happens within about 30 seconds for all trials.

Figure 3 shows all the raw data collected for 10% SOC overlaid for comparison. It can be seen that the battery returns to an equilibrium state for all pulse discharge times and C-rates within 240 seconds. Additionally, we can see that regardless of pulse discharge length and C-rate, the battery returns to approximately the same OCV. The 10% SOC trials had the most difference in ending voltage, which was limited to 25 mV. Considering that at low SOC, the OCV changes
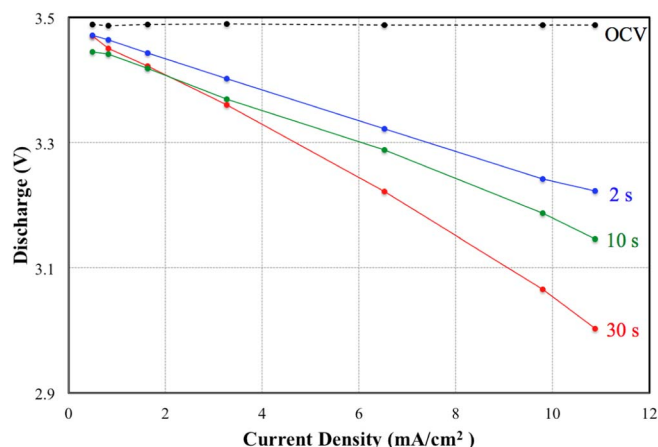
Figure 5. 10% SOC Pulse Polarization Curve created from the pulse discharge experiments.

dramatically as the battery is discharged towards 0% SOC, these results show impressive accuracy for the method presented.

The 40% and 70% SOC pulse discharge trials show similar trends to the 10% SOC data for relaxation time periods, with a notable difference. During the 30 second discharge, the slope of the curve is nearly straight in the 10% SOC experiments. For the 40%, and the 70% SOC 30 second trials, the curve is increasingly convex at high C-rates.

The experimental data collected for the 40% SOC exhibits better accuracy than that seen at 10% SOC. The maximum variance in OCV measured at 40% SOC is less than 15 mV, compared to 25 mV for 10% SOC data. This was attributed to the more gradual change in OCV slope at 40% SOC than 10% SOC.

LIB pulse polarization curves.—As explained previously, the voltage of the battery is recorded at the end of the pulse discharge to generate a point on the PPC. All of the pulse discharge trials relax to the same OCV after the current interrupt, therefore each point can be compared on the same graph at a given SOC. Separate PPCs are generated for each distinct SOC. Additionally, distinct PPCs are observed for each pulse discharge time, as seen in Figures 5–8. Figures 5–7 are the PPCs at 10%, 40%, and 70% SOC, respectively, for the large pouch cell. Figure 8 is the PPC for the small coin cell at 40% SOC.

In Figure 5, the pulse discharge curves illustrate the voltage vs. current density relationship at 10% SOC. The data show that the
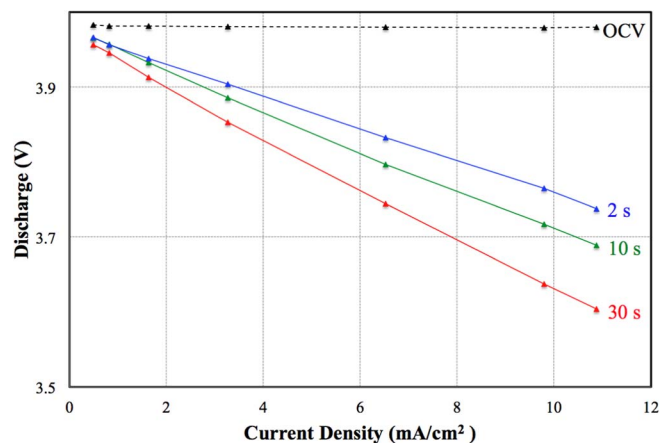
voltage losses experienced by the battery during operation increases as the current density increases and pulse discharge time lengthens. This is attributed to a Li$^+$ concentration gradient being more pronounced, and having a longer time to form respectively. Figures 6–8 also exhibit the same overall trends as those discussed for Figure 5, but shifted by their OCV for their respective SOC.

In Figures 6 and 8, the green and purple lines show the 10 seconds pulse discharge for 40% SOC, respectively. While both exhibit a linear trend, the current density experienced by the small coin cell is almost double to that applied to the large pouch cell. This is in spite of a lower maximum C-rate of 2 C being applied to the small coin cell, as opposed to a maximum of 20/3 C applied to the large pouch cell. This difference in C-rate vs. current density comparisons will be discussed later. A comparison of Figures 6 and 8 shows that this PPC method can be performed on batteries of various sizes and chemistries.

Comparing the PPCs in Fig. 5 to those of Figs. 6 and 7 shows that the overall voltage loss at high current density and long discharge time is higher for the 10% SOC data than for the 40% or the 70% data. This is clearly shown in Figure 9 where for the same pulse discharge times and currents the Li$^+$ concentration gradient in the electrolyte should also be the same. For these similar pulse discharges, the charge transfer kinetic voltage losses and the solid-state diffusion voltage losses are the only loss factors that change with SOC.

As seen in Figure 9, the voltage losses experienced by the battery at 40% and 70% SOC are nearly equal, while the voltage loss experienced by the battery at 10% SOC diverges at higher current densities

Figure 7. 70% SOC Pulse Polarization Curve created from the pulse discharge experiments.
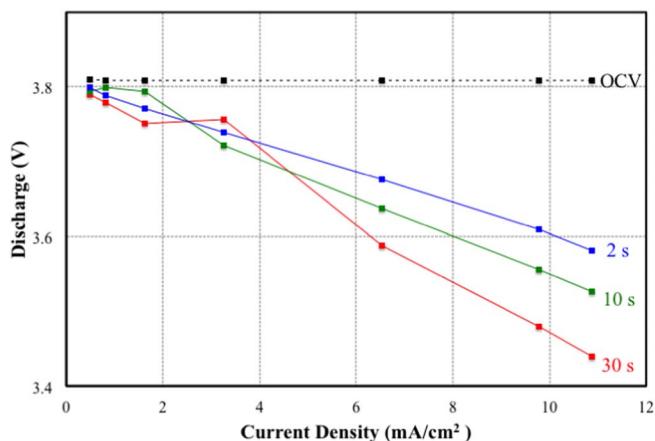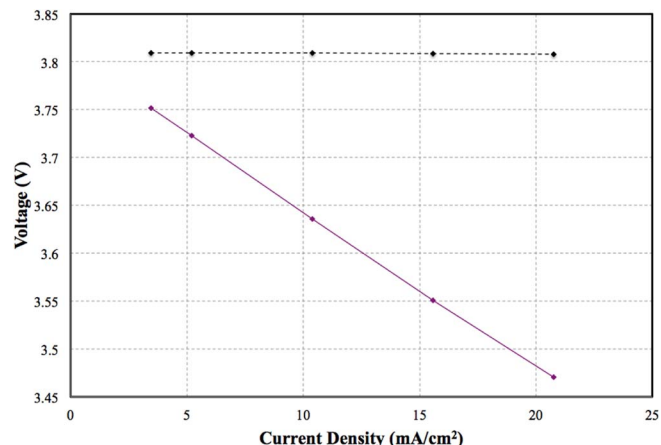

Figure 6. 40% SOC Pulse Polarization Curve created from the pulse discharge experiments.

Figure 8. Coin Cell 40% SOC Pulse Polarization Curve created from the 10 second pulse discharge experiments.
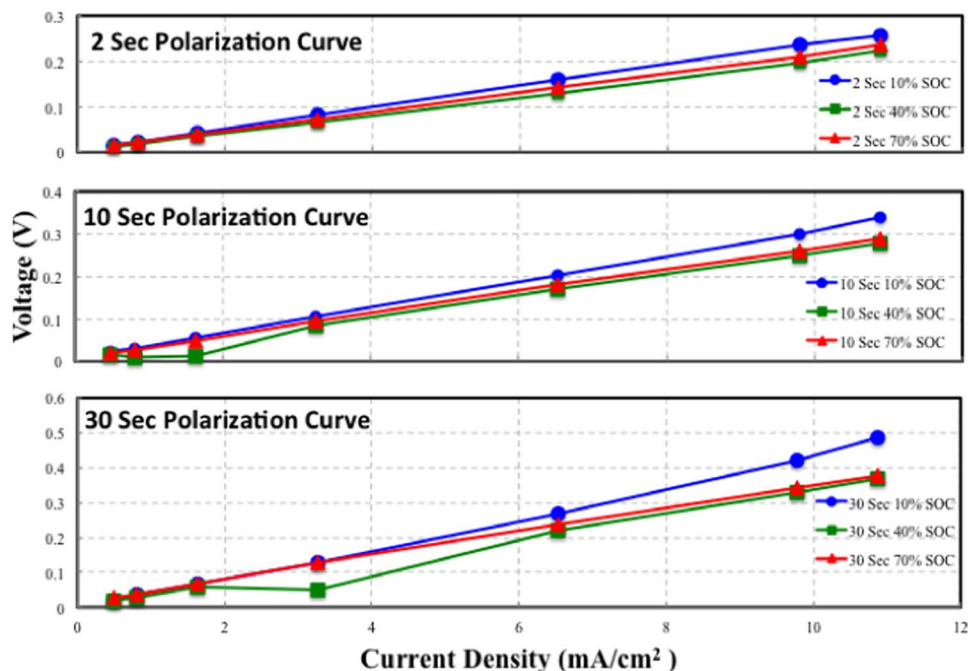
Figure 9. The voltage losses experienced at each pulse discharge and SOC are compared in this figure. As the pulse discharge lengthens and current density increases, the 10% SOC data has a higher voltage loss than that seen in the 40% and 70% SOC cases at 7 mA/cm^2 and above.

and pulse discharge times. There is increased voltage loss, and decreased battery performance, as the SOC of the battery decreases to 10% SOC.

C-rate vs. current density results.—It is interesting to compare batteries of similar C-rates or at similar current densities. While C-rate expresses the rate of discharge, current density expresses the flux, which is the rate per unit area. C-rate relates the rate of discharge to the capacity of the battery (in Ah). However, the current density cannot be calculated from the capacity unless the total area of the battery is given. It is therefore suggested to define a specific C-rate, which is the C-rate per unit area as defined by:

$$Specific \ C - rate = \frac{C_a C_C}{(Ah) \ A} \qquad [3]$$

where C_a is the applied current per cell, C_C is the constant current for a 1 hour discharge, A is the area of the electrodes, and Ah is the nominal capacity of the battery. Comparing under the same Specific C-rate would ensure the same current density between differing batteries for accurate performance characterization.

We compared C-rates and current densities for different battery chemistries and sizes, as shown in Figure 10. All pulse discharges were performed at 40% SOC and a pulse time of 10 seconds. The pulse discharge in red is for the coin cell at 1 C-rate. The pulse discharge in green is for the pouch cell at 1 C-rate, and the pulse discharge in blue is for the pouch cell at 20/3 C-rate.

When comparing the same C-rates, the pulse discharge for both pouch and coin cells also exhibit the same shaped convex curves. While the C-rate was the same when comparing the green and red curves in Figure 10, the current density of the coin cell was 10.39 mA/cm^2 while the current density of the pouch cell was 1.64 mA/cm^2. For the 1 C rate pulse discharges, the relaxation after the pulse is less than 1 second. This corresponds with kinetic and ohmic resistance, with a small amount of loss due to the Li$^+$ concentration gradient in the electrolyte.

When we compare equivalent current densities, the ohmic and kinetic voltage loss appears similar, but the pulse discharge curves have significantly different slopes. The relaxation period after the pulse discharge for the large pouch cell (blue line) was 30 seconds

vs. less than a second for the small coin cell. It indicates that the capacity of the battery (thickness of the electrodes) affects the pulse discharge behavior. The coin cell electrodes were estimated to be 10 times thicker than the electrodes found in the pouch battery, based on the 10 times difference in Ah/m^2 per unit cell. From this, we know that the coin cell was designed for higher energy density, while the pouch cell was designed for higher power density.

Discussion

Pulse Discharge Discussion.—The results of the pulse discharge method appear to experimentally separate various overvoltages in a battery's voltage performance. As shown in the pulse discharge experiments, the charge transfer kinetic, Li$^+$ ionic mass transport, and Li solid-state diffusion losses were partially separated by utilizing different pulse discharge times and examining the relaxation curves. As previously mentioned, different pulse durations were selected in
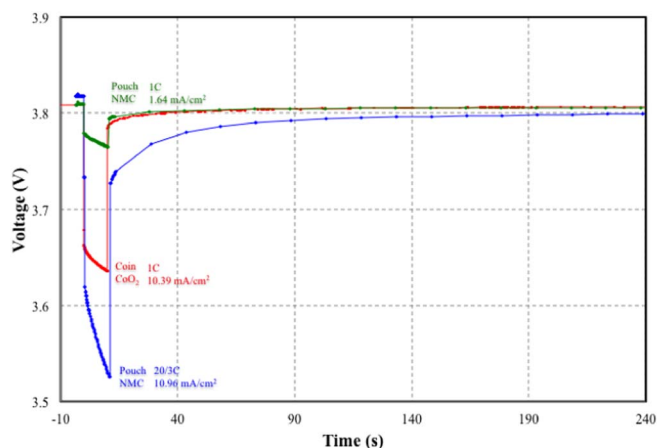

Figure 10. Comparison of pulse discharge results for a 10 second pulse discharge at 40% SOC for LiCoO$_2$ small coin cell and LiNiMnCoO$_2$ large pouch cell.

order to extract the charge transfer kinetic losses,[21,22] electrolyte Li+ mass transport losses,[23–30] and Li solid-state diffusion losses[31–42] by exploiting the fact that these phenomena develop at different time scales.

Voltage losses attributed to kinetics[14–18] occur on the order of 1 ms, as estimated from Eq. 1 where the length is determined by the SEI thickness[17–18] of 10 nm and diffusivity is 1.0 e^{-9} cm^2/s for the electrode active solid particles. The 2 seconds pulse discharge time relates to the intercalation/ de-intercalation of Li+ at the interface of the electrode active materials, or charge transfer kinetic voltage losses. At these time scales, it is assumed that concentration gradients do not have sufficient time to form in the electrolyte or within active particles, and only Li+ immediately adjacent to the active particles are used during the pulse.

The characteristic time for Li+ concentration gradient formation in the electrolyte[19,20] is between 5 and 10 seconds based on Eq. 1 where a diffusion length of 40–55 microns based on the electrode and separator thicknesses and a diffusivity of 3.0 10^{-6} cm^2/s for the electrolyte. Therefore at a pulse length of 10 seconds, we assume that a concentration gradient of Li+ ions has fully formed within the electrolyte of the battery being tested, but the solid-state diffusion has not changed significantly.

The characteristic diffusion time for Li diffusing in the electrodes[19,20] is between 20–200 seconds based on Eq. 1 using a half cell estimated diffusivity of 2.0 10^{-9} to 2.0 10^{-8} cm^2/s and a measured solid particle radius of 8 microns. The 30 seconds pulse discharge time relates to the Li solid-state diffusion in the electrodes active materials. However, at this time scale the Li concentration gradient has not yet fully formed in the active particles in the electrodes.

For the 2 second pulse discharge at 10% SOC, the relaxation to OCV occurs within 2 seconds of the current interrupt. If the voltage loss experienced by the battery during the pulse discharge was purely related to electronic ohmic and charge transfer kinetic losses, we would expect the relaxation period to be closer to 1 ms. Therefore we attribute 213 mV of the recovery to these losses, as this is the voltage recovery within 0.5 seconds of the pulse discharge ending. From 0.5 to 2 seconds after the pulse, the voltage recovers by 19 mV, which is likely due to the formation of a Li+ concentration gradient within the battery's electrolyte during the 2 second pulse discharge time. This was expected since 2 seconds is longer than the 1 ms characteristic time predicted for the charge transfer kinetic loss development. However, the 2 second relaxation time is shorter than the 5–10 seconds relaxation time expected for a fully developed Li+ concentration gradient in the electrolyte. From this, we can say that for the 2 seconds pulse discharge time, a Li+ concentration gradient has begun forming in the electrolyte, but has not achieved a steady-state. From 2 to 18 seconds the voltage increases by 12 mV, which we believe that the 2 to 18 second relaxation time is mostly due to the partially formed Li+ concentration gradient in the electrolyte, with a negligible amount of voltage loss due to Li solid-state diffusion losses.

Based on this analysis, we believe that the pulse discharge method has successfully captured voltage losses in the battery due mostly to charge transfer kinetic and ohmic resistive losses. A small amount of voltage loss is due to a Li+ concentration gradient in the electrolyte, but a negligible amount of voltage loss is due to solid-state diffusion of Li in the electrode particles. This is also true for the 40% and 70% SOC results at the 2 seconds pulse discharge times.

For the 10 seconds pulse discharge times, the relaxation time after the pulse discharge ranges from 2 seconds to 40 seconds. It is expected that a Li+ concentration gradient in the electrolyte alone would fully relax within 5–10 seconds. While C-rates at or below 2 C exhibit this expected result, the pulse discharge relaxation times for higher C rates all have relaxation periods of 20–40 seconds, increasing as the C-rate increases. Consequently, we believe that the 10 seconds pulse discharge has ohmic, charge transfer kinetic, ionic mass transport, and solid-state diffusion voltage losses since the relaxation period is longer than 5–10 seconds expected for electrolyte relaxation alone.

Analysis of the 20/3 C rate for the 10% SOC trials show that 247 mV of relaxation occurs within 0.5 seconds, 50 mV of relaxation occurs between 0.5 and 17.5 seconds, and 22 mV of relaxation occurs from 17.5 seconds to 47.5 seconds. We can attribute these voltage losses to: charge transfer kinetic and ohmic losses, Li+ concentration gradient in the electrolyte, and Li concentration gradient in solid-state diffusion, respectively.

We believe that the 10 seconds pulse discharge time successfully captures the Li+ concentration gradient in the electrolyte. The voltage losses attributed to the Li solid-state diffusion are likely present for this pulse discharge time, given that the relaxation period is discernibly longer than 10 seconds which is expected for the electrolyte relaxation. The 22 mV of relaxation seen from 17.5 to 47.5 seconds after the pulse discharge is smaller than the difference of 25 mV for the OCV, and therefore solid-state diffusion is not a measurable contributing factor for the 10 seconds pulse discharge. This analysis is also supported by the data for the 10 second pulse discharge times at 40% and 70% SOC.

The results for the 30 second pulse discharge experiments show that the separation of the voltage losses are as follows for the 10% SOC trials; 262 mV of relaxation is within 0.5 seconds, 40 mV of relaxation is from 0.5 to 2 seconds, 92 mV of relaxation is from 2 to 18 seconds, and 33 mV of relaxation is from 18 to 33 seconds after the pulse discharge. As described above, we attributed the 262 mV of relaxation to the charge transfer kinetic and ohmic voltage losses, and 40 mV to Li+ concentration gradient relaxation in the electrolyte. For the 30 seconds pulse discharge, we believe that the 92 mV relaxation seen between 2 and 18 seconds after the current interrupt is partially attributable to the Li+ concentration gradient in the electrolyte as well as Li concentration gradient existing in the solid-state diffusion of the active electrode particles. The 33 mV of voltage recovery that occurs from 18 to 33 seconds is within the range that solid-state diffusion voltage losses were expected.

A 24 mV change in potential was seen between 240 seconds and 1800 seconds. Another mechanism might be at work to account for this 24 mV difference in potential, as the characteristic diffusion time of the active electrode particles is 20–200 seconds as calculated from equation 1. Since 1800 seconds is nine times longer than the characteristic diffusion time, solid-state diffusion cannot account for this difference. Lithium diffusion through the electrode thickness between active particles to reduce a concentration gradient through the electrode thickness is therefore the most likely mechanism for this potential difference. However, since the OCV difference at 240 second is 25 mV, and the difference from 240 to 1800 seconds is within this value, it was deemed inconclusive or negligible.

The investigation of different pulse discharge times and their relaxation curves has shown that it is possible to partially separate coupled multiphase interactions using a pulse discharge method. This is encouraging, since there is a lack of tools to examine the effective component impact of operational cells such as individual overvoltages on overall battery performance. One recently introduced method[45] uses an acoustic wave passing through a battery to evaluate structure and SOC. In contrast, the results of this work demonstrate that a pulse discharge method can effectively match the ending SOC and isolate individual overvoltages within a battery. This is a necessary feature for the pulse discharge method to have in order to move to the next step, the creation of PPCs. Since battery performance depends on SOC, a difference in ending SOC would mean the PPC would compare voltage losses for different battery performance criteria. Being able to compare the voltage losses at the same SOC enables the creation of a PPC, which can in turn be utilized to analyze parameters governing battery performance across a range of conditions. From this analysis it can be determined whether kinetic, ohmic, or mass transport limitations primarily govern battery performance for a given current density and SOC.

Pulse polarization curve discussion.—The linear slope of the PPCs most closely resembles the region where ohmic resistance is the governing loss term. This indicates that for the current densities

and pulse discharge times tested in this work, kinetic and solid-state diffusion are not the dominant factors that limit discharge current. Furthermore, we can infer this since in a fuel cell polarization curve the operating conditions governed by kinetic loss have a convex shape and the operating region governed by mass transport has a concave shape.[8]

The voltage losses at longer pulse discharge times are, as a whole, governed by ohmic resistance. However, we can attribute voltage loss within specific time frames to individual mechanisms other than ohmic resistance.

The voltage losses for the 2 seconds pulse discharge should be mostly due to ohmic and kinetic loss relating to ohmic resistance, and the intercalation/ de-intercalation of Li^{+} into and out of the cathode and anode, respectively. As discussed in the previous section, there is evidence that the 2 seconds pulse discharge also has some voltage loss due to a Li^{+} concentration gradient existing in the electrolyte, so the 2 second PPC has some voltage loss attributed to this as well. The increase in voltage loss seen from the 2 to the 10 second PPC can be attributed to a more developed Li^{+} concentration gradient in the electrolyte. The difference between the 10 and 30 second PPC is attributed to the formation of a Li concentration gradient in solid-state diffusion within the active electrode particles.

Since pulse discharges can be performed on rechargeable batteries, a PPC can likewise be created for these batteries, independent of chemistry and construction. In this way, comparisons of voltage loss between battery components and chemistries can be ascertained at a system level. This would also capture component interactions not separately measurable. In this way, the pulse discharge method will yield more relevant results regarding cell operation and performance than separate component measurements allow.

As shown in Figure 9, when we kept pulse discharge time and current density constant, we found increased voltage loss at low SOC. One possible reason for the increase in voltage loss at 10% vs. 40% and 70% SOC, is due to the reduced amount of Li in the negative electrode. While there is also an argument that the loss could be attributed to the positive electrode since it is 90% filled, we believe the negative electrode is the cause of the decreased performance at 10% SOC. This is due to the increased diffusion length from the center of the active particles for Li at concentrations lower than LiC_{27} in the solid-state active particles of the negative electrode, compared to Li diffusing into the solid-state active particles of the positive electrode. Additionally, the $X^{1/2}(1-X)^{1/2}$ stoichiometry[X] for determining the exchange current density i_0 is 0.299 and 0.280 for the positive and negative electrode, respectively for 10% SOC, so the local current density is equivalent for both electrodes. Therefore, the difference seen in overall voltage loss in the electrodes is not attributed to kinetic charge transfer losses, and is believed to be solid-state diffusion related.

The electrodes in the lithium-ion battery can be thought of as two connected Li reservoirs. As the amount of Li in the anode reservoir decreases, the rate is reduced because it becomes harder and harder to remove additional lithium ions from the graphite in the anode. This can be seen as the SOC decreases to 10% SOC in Figure 9.

Conversely, during discharge the cathode reservoir is accepting lithium ions, and therefore during discharge, the rate at which lithium ions arrive is independent of the cathode content, but dependent on the anode. Therefore the cathode appears to exhibit very little SOC dependence for the SOC's that we tested. This is in contrast to the case when the performance is affected by the contents of both electrodes. As the anode releases Li^{+}, it becomes more difficult for the cathode to accept Li^{+}.

C-rate vs. current density comparison.— When comparing C-rate vs. current density as the metric to measure battery performance, different mechanisms are being compared. Based on our results, it appears that C-rate determines charge transfer kinetic and ohmic losses. Current density determines ionic mass transport and solid-state diffusion losses.

When comparing at the same C-rate between the small and large batteries, as seen in Figure 10 for the green and red curves, there

is a shift in voltage loss that appears to be ohmic and kinetic loss in nature, since the relaxation period is nearly instantaneous. It is therefore unlikely to be related to electrolyte mass transport or solid-state diffusion.

When comparing at the same current density, as shown in Figure 10 for the red and blue curves, the differences between the battery performances are mostly due to electrolyte mass transport and solid-state diffusion, since the relaxation period is 30 seconds. It is believed that most of the recovery is due to the Li^{+} concentration gradient in the electrolyte returning to equilibrium. Since the recovery period is greater than 10 seconds it is likely that there is a concentration gradient in the active particles of the electrodes as well.

We believe that the relaxation of the voltage beyond 200 seconds is due to a Li concentration gradient forming through the thickness of the electrodes. This mechanism is the most likely since a concentration gradient within the active particles would recover within 200 seconds, while a concentration gradient between particles would equilibrate over a longer period.

In evaluating the small vs. large battery, the Li^{+} specific capacities are 10.2 mAh/cm^{2} and 1.64 mAh/cm^{2} for the two batteries respectively. Since the specific capacity is different, the differences in relaxation times seen in Figure 10 are likely due to electrode thickness. We have attributed the voltage differences in Figure 10 for similar C-rate and current densities to ohmic and charge transfer kinetic, or ionic mass transport and solid-state diffusion respectively.

Conclusions

We described a pulse discharge method for measuring battery performance at the same ending SOC, and why this is important for accurate battery performance metrics. Since there is a SOC dependence on battery performance, to compare performance the end of the pulse discharge needed to be at the same SOC. Additionally, to later construct PPCs, all pulse discharges needed to end at the same SOC for the same reason. This was done for both a large pouch (15 Ah) and a small coin (0.032 Ah) battery to establish the reproducibility of this method on both a large and small scale.

The results of the pulse discharge experiments suggest that kinetics are captured in the 2 second pulse discharge time. Electrolyte Li[+] concentration gradient and Li solid-state diffusion are established in the 10 and 30 seconds pulse discharge times, respectively. While the beginning of Li diffusion concentration gradient in the solid-state active electrode particles can be captured using a 30 second pulse discharge, longer times are needed to analyze a fully formed Li concentration gradient in the active electrode particles.

Utilizing the results of the pulse discharge experiments, PPCs were created and the portions of the polarization curve dominated by ohmic, kinetic and solid-state diffusion have been identified. We also noted a greater voltage loss for 10% SOC than for 40% and 70% SOCs tested. We attributed this finding to a low Li ion concentration in the negative electrode.

We evaluated C-rate vs. current density as metrics for battery performance in different size batteries and chemistries. C-rate is better for comparing ohmic and kinetic voltage loss contribution differences, while current density is better for comparison of mass transport voltage losses.

Acknowledgments

List of Symbols

A	Area of the electrodes, cm^2
Ah	Nominal Capacity of the battery, Ah
C	Capacity of the battery, Ah
C_a	Applied current per cell, A
C_C	Constant current for a one hour discharge, A
D	Diffusion coefficient, cm^2/s
I	Current of pulse discharge, A
L	Characteristic diffusion length, m
SOC_{start}	SOC at beginning of pulse discharge, %
SOC_{end}	SOC at end of pulse discharge, %
t	Length of pulse discharge, s

Greek

τ_s	Characteristic diffusion time, s

Subscripts and Superscripts

a	Applied
C	Constant
end	End of pulse
s	Time
$start$	Beginning of pulse

References

1. T. Fuller, M. Doyle, and J. Newman, *J. Electrochem. Soc.*, **141**, 1 (1994).
2. M. Doyle and J. Newman, *J. Electrochem. Soc.*, **143**, 6 (1996).
3. D. Bernardi and J.-Y. Go, *J. Power. Sour.*, **196**, 412 (2011).
4. A. G. Hseih, S. Bhadra, B. J. Hertzberg, P. J. Gjeltema, A. Goy, J. W. Fleischer, and D. A. Steingart, *Energy Environ., Sci.*, **8**, 1569 (2015).
5. S. Wijewardana, R. Vepa, and M. H. Shaheed, *J. Power. Sour.*, **308**, 109 (2016).
6. J.-N. Shen, Y.-J. He, and Z.-F. Ma, *AIChE Journal*, **62**, 78 (2015).
7. Z. Yu and R. N. Carter, *J. Power Sour.*, **195**, 1079 (2010).
8. J. Larminie and A. Dicks, "*Fuel Cell Systems Explained*," England, John Wiley & Sons, Inc. (2003).
9. M. Whittingham, *Chem. Rev.*, **104**, 4271 (2004).
10. T. DuBeshter, P. K. Sinha, A. Sakars, G. W. Fly, and J. Jorne, *J. Electrochem. Soc.*, **161**, A599 (2014).
11. K.-W. Nam, W.-S. Yoon, H. Shin, K. Y. Chung, S. Choi, and X.-Q. Yang, *J. Power Sour.*, **192**, 652 (2009).
12. *J. Power. Sour.*, **196**, 7039 (2011).
13. I. V. Thorat, D. E. Stephenson, N. A. Zacharias, K. Zaghib, J. N. Harb, and D. R. Wheeler, *J. Power Sour.*, **188**, 592 (2009).
14. J. Bisquert, *Electrochimica Acta*, **47**, 2435 (2002).
15. J. Bisquert and V. S. Vikhrenko, *Electrochimica Acta*, **47**, 3977 (2002).
16. P. Lu and S. J. Harris, *Electrochem. Comm.*, **13**, 1035 (2011).
17. E. Peled and H. Yamin, *Israel Journal of Chemistry*, **18**, 131 (1979).
18. E. Peled, *J. Electrochem. Soc.*, **126**, 2047 (1979).
19. P. Albertus, J. Christensen, and J. Newman, *J. Electrochem. Soc.*, **156**, A606 (2009).
20. P. Albertus et al., *J. Power Sour.*, **183**, 771 (2008).
21. K. Dokko, M. Mohammedi, M. Umeda, and I. Uchida, *J. Electrochem. Soc.*, **150**, A425 (2003).
22. S. Bach, J. P. Pereira-Ramos, and P. Willmann, *Electrochimica Acta*, **56**, 10016 (2011).
23. S. G. Stewart and J. Newman, *J. Electrochem. Soc.*, **155**, F13 (2008).
24. L. O. Valoen and J. N. Reimers, *J. Electrochem. Soc.*, **152**, A882 (2005).
25. J. Newman, D. Bennion, and C. W. Tobias, *Sonderdruck aus der Zeitschrift*, **69**, 608 (1965).
26. H. Hafezi and J. Newman, *J. Electrochem. Soc.*, **147**, 3036 (2000).
27. H. Dai and T. A. Zawodzinski, *J. Electroanalytical Chem.*, **459**, 111 (1998).
28. J. Zhao, L. Wang, X. He, C. Wan, and C. Jiang, *J. Electrochem. Soc.*, **155**, A292 (2008).
29. C. Capiglia, Y. Saito, H. Yamamoto, H. Kageyama, and P. Mustarelli, *Electrochimica Acta*, **45**, 1341 (2000).
30. C. Capiglia, Y. Saito, H. Kageyama, P. Mustarelli, T. Iwamoto, T. Tabuchi, and H. Tukamoto, *J. Electrochem. Soc.*, **81–82**, 859 (1999).
31. J. P. Meyers, M. Doyle, R. M. Darling, and J. Newman, *J. Electrochem. Soc.*, **147**, 2930 (2000).
32. D. W. Dees, S. Kawauchi, D. P. Abraham, and J. Prakash, *J. Power Sour.*, **189**, 263 (2009).
33. W. Weppner and R. A. Huggins, *J. Electrochem. Soc.*, **124**, 1569 (1977).
34. D. P. Abraham, S. Kawauchi, and D. W. Dees, *Electrochimica Acta*, **53**, 2121 (2008).
35. H. Yang, H. J. Bang, and J. Prakash, *J. Electrochem. Soc.*, **151**, A1247 (2004).
36. M. D. Levi, K. Gamolsky, D. Aurbach, U. Heider, and R. Oesten, *J. Electroanalytical Chem.*, **477**, 32 (1999).
37. P. Yu, B. N. Popov, J. A. Ritter, and R. E. White, *J. Electrochem. Soc.*, **146**, 8 (1999).
38. S. Harris, A. Timmons, D. R. Baker, and C. Monroe, *Chem. Phys. Let.*, **485**, 265 (2010).
39. Y. Zhu and C. Wang, *J. Phys. Chem.*, **114**, 2830 (2010).
40. E. Markevich, M. D. Levi, and D. Aurbach, *J. Electroanalytical Chem.*, **580**, 231 (2005).
41. M. Park, X. Zhang, M. Chung, G. B. Less, and A. M. Sastry, *J. Power Sour.*, **195**, 7904 (2010).
42. K. Persson et al., *J. Phys. Chem. Let.*, **1**, 1176 (2010).
43. Li-ion battery LIR2032, *AA Port. Power. Co.*, (2006), February 23.
44. E. Markevich, M. D. Levi, and D. Aurbach, *J. Electro. Chem.*, **580**, 231 (2005).
45. A. G. Hseih, S. Bhadra, B. J. Hertzberg, P. J. Gjeltema, A. Goy, J. W. Fleischer, and D. A. Steingart, *Energy Environ., Sci.*, **8**, 1569 (2015).
46. T. DuBeshter, J. Jorne, Polarization for Li-Ion Battery Under Constant State of Charge: II. Modeling and Separation of Individual Voltage Losses, *J. Electrochem. Soc.*, submitted, (2017).
47. T. DuBeshter, Pulse Polarization for li-Ion Battery Under Constant State of Charge, PhD dissertation, University of Rochester, (2016).